Supporting Online Material for

Experimental Realization of a Magnetic Cloak

Fedor Gömöry, Mykola Solovyov, Ján Šouc, Carles Navau, Jordi Prat-Camps, Alvaro Sanchez*

*To whom correspondence should be addressed. E-mail: alvar.sanchez@uab.cat

Published 30 March 2012, *Science* **335**, 1466 (2012)
DOI: 10.1126/science.1218316

This PDF file includes:

Materials and Methods

Finite-element calculations for simulating non-ideal materials

Because of the employed superconductor and ferromagnetic materials, some non-ideal behavior would be expected. In order to quantify these effects we have performed finite-element calculations under the following assumptions:

- The structure is infinite along its cylindrical axis (this means two-dimensional distributions of currents and fields have been computed).

- Superconductor behaves according to the critical state model (*27*) - this approximation is widely used for high-temperature superconductors with strong pinning of magnetic flux working at 77 K in quasi-static conditions (frequencies below 1 kHz).

- Magnetic permeability of ferromagnetic material is finite and isotropic.

The calculation procedure has been developed earlier for the purpose of investigating the possibility to improve the transport capability of a superconducting wire with the help of a ferromagnetic layer (*28*). It provided excellent predictions for the electromagnetic properties of high-temperature tapes with ferromagnetic substrate (*29*). As an example Fig. S1 shows the distribution of magnetic field in the magnetic cloak shell with number of layers n_{SC} = 2 and n_{FM} = 7 at switching on the uniform magnetic field of 40 mT. Magnetic invisibility of the magnetic cloak is evident - a deformation of straight induction lines is hardly observable.

Quantitatively, the effect of combining SC and FM materials is illustrated by the calculated results in Fig. S2 showing the scan of the vertical component of magnetic induction B_{y} at a fixed height above the two-shell cloak (along the dashed line in Fig. S1).

The properties of materials entering the calculations have been derived from independent tests. From the critical current of the 12 mm wide tape measured at 77 K the critical current density in a superconducting layer of supposed thickness 1 μm was evaluated as J_{c} = 3 $\times$ 10^{10} A/m^2. This property characterizes the transport capability along the tape length i.e. in circumferential direction in our geom-

etry shown in Fig. S1. When putting this value in our simulations the results predicted much stronger screening than observed experimentally. Eventually, nice agreement was achieved when assuming J_c = 10^{10}A/m^2. Such difference can be explained by the combination of several factors. First, the currents securing the cloaking effect flow in direction perpendicular to the drawing plane of Fig. S1 (along z-coordinate) that is across the tape width and commercial tapes are not optimized for this direction of current. Even more significant is the fact that all the screening current must change direction at the ends of a finite tubular cloak. This flow of current - particularly limiting in our case of L comparable to ϕ_{in} - happens along the tape edges, well known for being the place of a reduced critical current. We believe these end effects cause the observed reduction of transport capability by factor 3 compared to a straight tape.

The magnetic permeability of the FeNiCr tape was measured on a toroidal sample made of 3 turns. In wide scale of excitation fields the relative permeability ranged between 11 and 18. The difference in predicted distributions obtained assuming these limiting values was negligible.

Construction of the bilayer

A 1 μm thick layer of cuprate superconductor ReBCO deposited on 100 μm metallic substrate (*20*) is able to carry without resistance the electrical current exceeding 400 A in 12 mm wide tape when cooled by liquid nitrogen to the temperature of 77 K. Changing the number of turns the tape has been wrapped around the central bore, n_{SC}, allows to vary the strength of magnetic field expulsion. An outer shell with the task of sucking the magnetic flux expelled from central bore is wound from 100 μm thick $Fe_{18}Cr_9Ni$ alloy sheet. With the number of FM turns, n_{FM}, we can adjust the magnetic response of the outer shell. Thickness of this tape is another free parameter of the geometry.

On the cylindrical mandrel from textile-reinforced plastic two turns of superconducting tape 12 mm wide were first wrapped. To avoid uncontrolled short-circuiting of the turns, 70 μm thick kapton layer was inserted between them. Secondly, from the sheath of FeNiCr alloy a strip 12 mm wide was cut in

the length sufficient to wrap seven turns of this ferromagnetic material, alternated with a 215 μm thick kapton layer placed between them.

This exterior ferromagnetic part, consisting in an alternation of ferromagnetic layers (with measured permeability between 11 and 18) and kapton layers (with null magnetic contribution), would yield a decreased effective permeability much closer to the theoretical value of $\mu_2 = 3.5$ calculated with Eq. 1 using the final radii relation $R_2/R_1 = 1.34$ of the experimental set-up.

Preparation of the experimental bilayer

Both the high temperature superconductor and the ferromagnetic alloy used to manufacture the two shell structure exhibit some magnetic hysteresis. This means the magnetic profiles measured after various histories of applied field could differ. In the case of superconductor the remanent currents could be canceled by warming-up above the critical temperature. For the ferromagnetic material one can achieve a quasi-demagnetized state after application of a series of magnetic field pulses with alternating polarity and decreasing amplitude. We used both these measures to obtain in each of the above mentioned cases the profile corresponding to the history of applied field that is a simple change from zero to the desired value.

SOM text

Analytical derivation of cloaking behavior for a superconductor-magnetic cylindrical bilayer in uniform applied field

We consider a cylindrical shell (infinite in the z direction) of radii R_0 and $R_1 > R_0$ with uniform permeability μ_1 and another concentric cylindrical shell of radii R_1 and $R_2 > R_1$ with permeability μ_2. A uniform field H_a is externally applied in the y direction.

We want to calculate the magnetic field distribution in the whole space. Since no free currents are present, the magnetic field $\mathbf{H}$ can be written in terms of a magnetic scalar potential ϕ, $\mathbf{H} = -\nabla\phi$, that

should satisfy the Laplace equation $\nabla^2\phi = 0$ in all the regions of space. For the present geometry, the general solution of Laplace equation expressed in cylindrical coordinates, where θ is the angle with respect to the applied field direction, is (*30*)

$$\begin{aligned}\phi_i = a_{0,i} + b_{0,i}\ln\rho &+ \sum_1^\infty a_{n,i}\rho^n \sin(n\theta + \alpha_{n,i}) \\ &+ \sum_1^\infty b_{n,i}\rho^{-n}\sin(n\theta + \beta_{n,i}),\end{aligned} \tag{S1}$$

where $a_n, b_n, \alpha_n, \beta_n$ are constants to be determined by the boundary conditions and the subindex i stands for the different regions where ϕ is going to be determined: $i = 0$ for the region inside the hole ($\rho < R_0$), $i = 1$ for the inner layer ($R_0 < \rho < R_1$), $i = 2$ for the outer layer ($R_1 < \rho < R_2$), and $i = 3$ for the exterior region ($\rho > R_2$).

Taking into account that (a) ϕ_3 should tend to $-H_a\rho\cos\theta$ (the applied scalar potential) when $\rho \to \infty$, (b) ϕ_0 should be finite at $\rho = 0$, and (c) the standard magnetostatic boundary conditions must be obeyed, then one can find the scalar potential in all the regions. The final solutions can be expressed in the form

$$\phi_0 = F\rho\cos\theta, \tag{S2}$$

$$\phi_1 = \left(D\rho + \frac{E}{\rho}\right)\cos\theta, \tag{S3}$$

$$\phi_2 = \left(B\rho + \frac{C}{\rho}\right)\cos\theta, \tag{S4}$$

$$\phi_3 = \left(-H_a\rho + \frac{A}{\rho}\right)\cos\theta, \tag{S5}$$

where A, B, C, D, E, and F are the solutions of the following system of equations

$$BR_1^2 + C - DR_1^2 - E = 0, \tag{S6}$$

$$DR_0^2 + E - FR_0^2 = 0, \tag{S7}$$

$$-A - \mu_2 BR_2^2 + \mu_2 C = H_a R_2^2, \tag{S8}$$

$$A - BR_2^2 - C = H_a R_2^2, \tag{S9}$$

$$\mu_2 BR_1^2 - \mu_2 C - \mu_1 DR_1^2 + \mu_1 E = 0, \tag{S10}$$

$$\mu_1 D R_0^2 - \mu_1 E - F R_0^2 \;=\; 0, \tag{S11}$$

which can be analitically obtained. The general combination of positive permeabilities for the cylindrical case that yields a zero distortion of the applied field in the region $\rho > R_2$ is

$$\mu_2 = \frac{\mathcal{K}}{2(R_1^2 - R_2^2)[(1-\mu_1)R_0^2 - (1+\mu_1)R_1^2]} + \frac{\sqrt{4\mu_1[(1-\mu_1)R_0^2 - (1+\mu_1)R_1^2][(1-\mu_1)R_0^2 + (1+\mu_1)R_1^2](R_1-R_2)^2(R_1+R_2)^2 + \mathcal{K}^2}}{2(R_1^2 - R_2^2)[(1-\mu_1)R_0^2 - (1+\mu_1)R_1^2]}, \tag{S12}$$

where we have defined an auxiliary parameter

$$\mathcal{K} \equiv (\mu_1^2 - 1)(R_0^2 - R_1^2)(R_1^2 + R_2^2). \tag{S13}$$

As a particular case, when the inner layer is superconducting ($\mu_1 = 0$), the previous constants reduce to

$$A \;=\; H_0 R_0^2 \frac{(1+\mu_2)R_1^2 - (-1+\mu_2)R_2^2}{(-1+\mu_2)R_1^2 + (1-\mu_2)R_2^2}, \tag{S14}$$

$$C = R_1^2 B \;=\; \frac{2H_0 R_1^2 R_2^2}{(-1+\mu_2)R_1^2 - (1+\mu_2)R_2^2}, \tag{S15}$$

$$E = -R_0^2 D \;=\; \frac{4H_0 R_0^2 R_1^2 R_2^2}{(-1+\mu_2)R_1^2 - (1+\mu_2)R_2^2}, \tag{S16}$$

$$F \;=\; 0. \tag{S17}$$

In this case, by setting $A = 0$ in Eq. (S14) we obtain Eq. 1 of the main text

$$\mu_2 = \frac{R_2^2 + R_1^2}{R_2^2 - R_1^2}. \tag{S18}$$

Superconductor-magnetic spherical bilayer in uniform applied field

Analytical derivations can also be made for a spheric configuration, instead of a cylindrical one. A hollow sphere with a hole of radius R_0, an inner layer with radii R_0 and R_1 and permeability μ_1, and an outer

layer with radii R_1 and R_2 with permeability μ_2 ($R_0 < R_1 < R_2$) produces no external field distortion when

$$\mu_2 = \frac{\mathcal{P}}{4\left((-1+\mu_1)R_0^3+(1+2\mu_1)R_1^3\right)\left(R_1^3-R_2^3\right)} + \frac{\sqrt{-8\mu_1\left(2(-1+\mu_1)R_0^3-(1+2\mu_1)R_1^3\right)\left((-1+\mu_1)R_0^3+(1+2\mu_1)R_1^3\right)\left(R_1^3-R_2^3\right)^2+\mathcal{P}^2}}{4\left((-1+\mu_1)R_0^3+(1+2\mu_1)R_1^3\right)\left(R_1^3-R_2^3\right)}, \quad \text{(S19)}$$

where we have defined another auxiliary parameter

$$\mathcal{P} \equiv (-1+4\mu_1^2)R_1^6+(-2+\mu_1)(1+2\mu_1)R_1^3R_2^3-(-1+\mu_1)R_0^3((1+4\mu_1)R_1^3+2(1+\mu_1)R_2^3). \quad \text{(S20)}$$

Magnetic fields in all regions can be obtained analytically also in this case. When the inner layer is an ideal superconductor, the non-distortion in the exterior regions requires

$$\mu_2 = \frac{2R_2^3+R_1^3}{2(R_2^3-R_1^3)}. \quad \text{(S21)}$$

Although not directly related to our work, some derivations for the electric field in systems with coated spherical inclusions were presented in the context of the theory of composites (*31*,*32*). There, the goal was not to design cloaks but to find the effective conductivity for a composite comprised typically of spherical grains that did not distort an applied electric field. In (*33*), a discussion of the required dielectric constant values for a compound dielectric ellipsoids to reduce its scattering of electromagnetic radiation was presented.

Superconductor-magnetic cylindrical bilayer in non-uniform applied field

Here we discuss the cloaking behaviour of a superconductor-magnetic cylindrical bilayer when the applied field has some spatial variation. We provide a way to estimate the external field distortion and a general procedure to reduce it. The distortion zones showing where the magnetic induction $\mathbf{B}$ differs from the externally applied magnetic induction $\mathbf{B}_{\rm ext}$ in more than p per cent are calculated as the points in space where

$$\frac{\mid \mathbf{B}-\mathbf{B}_{\rm ext} \mid}{\mid \mathbf{B}_{\rm ext} \mid} > p/100. \quad \text{(S22)}$$

The magnetic response of a superconducting-magnetic bilayer to the fields of a single small magnet (basically a dipole field) at different distances from the bilayer are shown in Fig. S3, calculated by Comsol Multiphysics software, using the electromagnetics module (magnetostatics). In these cases of non-uniform applied field, a distortion of the external field occurs - distortion gets larger with increasing applied field inhomogeneity-, but it can be seen that this distortion is less than few percent in all space except in a region close to the field source and the bilayer. As an example, the dark pink region corresponding to a 5% distortion that in the case of a dipole at a distance $2.5R_2$ occupies a region of about 2-3R_2, extends to more than $15R_2$ in the case of a single magnetic layer or a single superconducting one (like those in Figs. 1, A and B).

There is an important effect worth to discuss. When *reducing* the thickness of the outer magnetic layer R_2, keeping R_1 constant and changing μ_2 according to Eq. 1, the region in which the external field is distorted is reduced. Actually, for thin magnetic layers, $R_2 - R_1 << R_1$, Eq. 1 reduces to $\mu_2 \simeq R_1/(R_2 - R_1)$. In that case, the large values of μ_2 allow a strong modification of the external field inside the thin layer. This effect is seen in Fig. S4, where the calculated distortion zone in the case of a near dipole, an unfavorable case in terms of field inhomogeneity, is clearly reduced by decreasing the thickness of the magnetic layer.

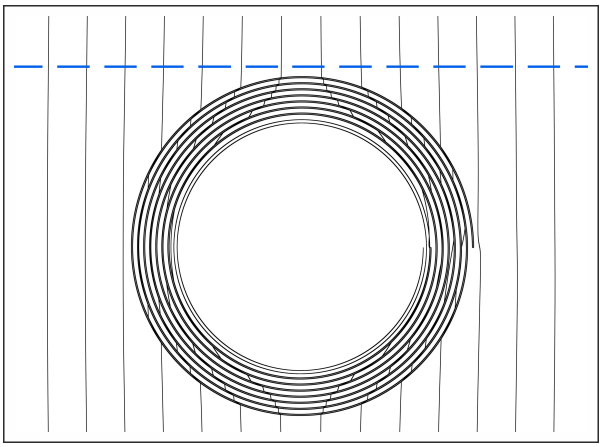

Figure S1: Example of 2D calculation for uniform magnetic field applied in perpendicular direction to the two-shell magnetic cloak (that is assumed infinite in the direction perpendicular to the drawing plane). Two inner turns are from superconducting material (thickness 1 μm), seven outer turns (thickness 100 μm) from ferromagnetic alloy.

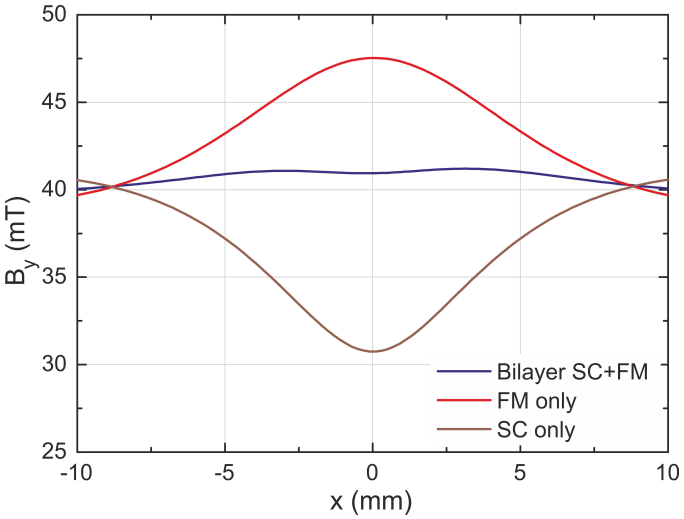

Figure S2: Calculated distribution of y-component of magnetic induction along the dashed line shown in Fig. S1 for applied field 40 mT, superconductor critical current density 10^{10} A/m^2, permeability of magnetic material μ_r = 11 (blue line). For comparison the calculated results are shown for the case of switched off superconductor (FM only) and non-magnetic ferromagnetic layers (SC only).

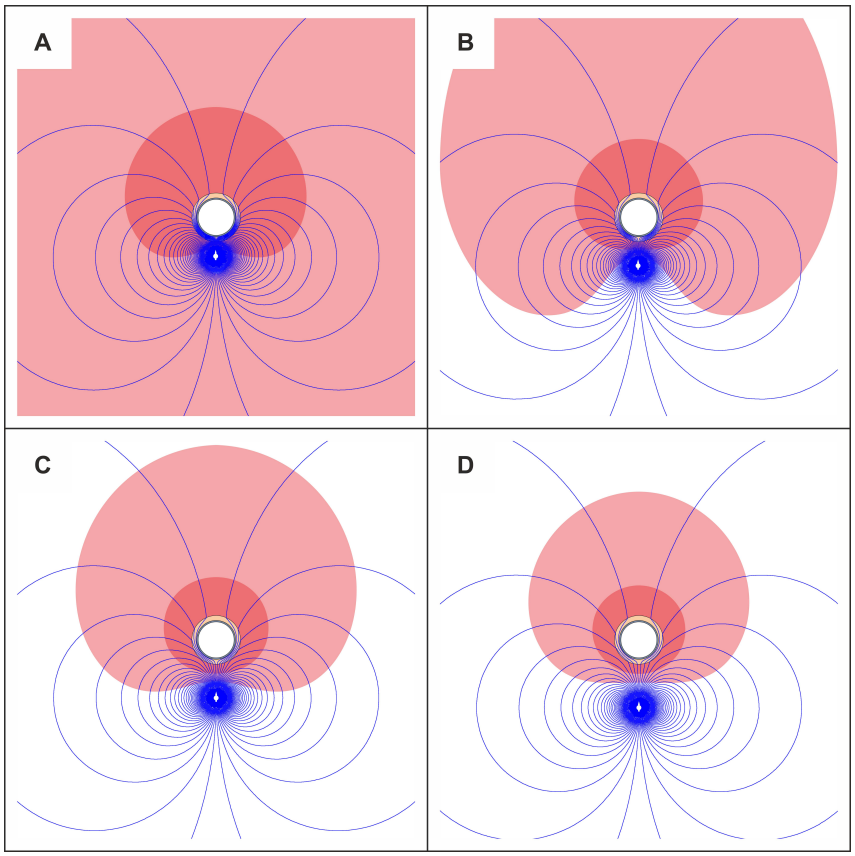

Figure S3: Calculated field lines for the interaction of a bilayer device (with $R_2/R_1 = 1.25$) with the field created by a magnetic dipole placed at different distances from the center of the device: (A) $2R_1$, (B) $2.5R_1$, (C) $3R_1$ and (D) $3.5R_1$. Bright (dark) pink-shaded regions indicate where distortion is larger that 1% (5%).

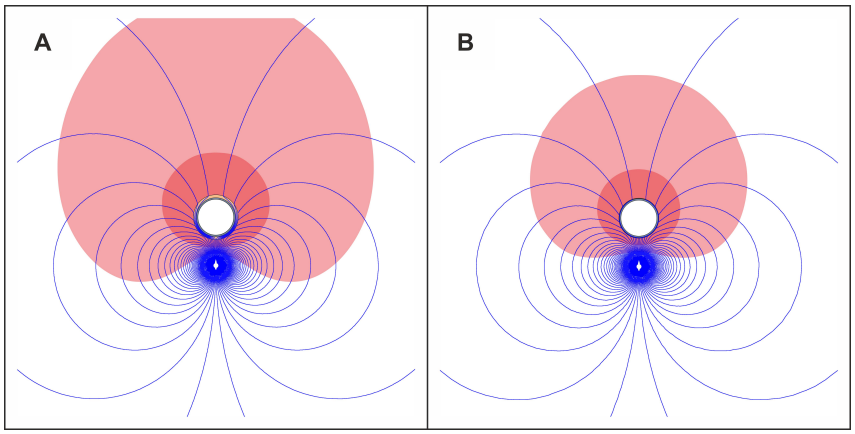

Figure S4: Calculated field lines and distortion regions for the interaction of a dipolar field (source is at a distance of $2.5R_1$ from the center of the bilayer) with bilayer devices with different thickness for the outer layer [(A) $R_2/R_1 = 1.15$, and (B) $R_2/R_1 = 1.025$], with corresponding permeabilities given by Eq. 1. Bright (dark) pink-shaded regions indicate where distortion is larger than 1% (5%).

References and Notes

1. J. B. Pendry, D. Schurig, D. R. Smith, Controlling electromagnetic fields. *Science* **312**, 1780 (2006). doi:10.1126/science.1125907 Medline

2. U. Leonhardt, Optical conformal mapping. *Science* **312**, 1777 (2006). doi:10.1126/science.1126493 Medline

3. A. Greenleaf, M. Lassas, G. Uhlmann, Anisotropic conductivities that cannot be detected by EIT. *Physiol. Meas.* **24**, 413 (2003). doi:10.1088/0967-3334/24/2/353 Medline

4. A. Alù, N. Engheta, Plasmonic and metamaterial cloaking: Physical mechanisms and potentials. *J. Opt. A Pure Appl. Opt.* **10**, 093002 (2008). doi:10.1088/1464-4258/10/9/093002

5. J. Perczel, T. Tyc, U. Leonhardt, Invisibility cloaking without superluminal propagation. *New J. Phys.* **13**, 083007 (2011). doi:10.1088/1367-2630/13/8/083007

6. P. Alitalo, F. Bongard, J.-F. Zürcher, J. Mosig, S. Tretyakov, Experimental verification of broadband cloaking using a volumetric cloak composed of periodically stacked cylindrical transmission-line networks. *Appl. Phys. Lett.* **94**, 014103 (2009). doi:10.1063/1.3068749

7. D. Schurig *et al*., Metamaterial electromagnetic cloak at microwave frequencies. *Science* **314**, 977 (2006). doi:10.1126/science.1133628 Medline

8. H. F. Ma, T. J. Cui, Three-dimensional broadband ground-plane cloak made of metamaterials. *Nat. Commun.* **1**, article 21 (2010). doi:10.1038/ncomms1023 Medline

9. B. Edwards, A. Alù, M. Silveirinha, N. Engheta, Experimental verification of plasmonic cloaking at microwave frequencies with metamaterials. *Phys. Rev. Lett.* **103**, 153901 (2009). doi:10.1103/PhysRevLett.103.153901

10. J. Li, J. B. Pendry, Hiding under the carpet: A new strategy for cloaking. *Phys. Rev. Lett.* **101**, 203901 (2008).

11. R. Liu *et al*., Broadband ground-plane cloak. *Science* **323**, 366 (2009). doi:10.1126/science.1166949 Medline

12. X. Chen *et al*., Macroscopic invisibility cloaking of visible light. *Nat. Commun.* **2**, article 176 (2011). doi:10.1038/ncomms1176 Medline

13. T. Ergin, N. Stenger, P. Brenner, J. B. Pendry, M. Wegener, Three-dimensional invisibility cloak at optical wavelengths. *Science* **328**, 337 (2010). doi:10.1126/science.1186351 Medline

14. B. Zhang, Y. Luo, X. Liu, G. Barbastathis, Macroscopic invisibility cloak for visible light. *Phys. Rev. Lett.* **106**, 033901 (2011).

15. B. Wood, J. B. Pendry, Metamaterials at zero frequency. *J. Phys. Condens. Matter* **19**, 076208 (2007). doi:10.1088/0953-8984/19/7/076208 Medline

16. F. Magnus *et al*., A d.c. magnetic metamaterial. *Nat. Mater.* **7**, 295 (2008). doi:10.1038/nmat2126 Medline

17. C. Navau, D.-X. Chen, A. Sanchez, N. Del-Valle, Magnetic properties of a dc metamaterial consisting of parallel square superconducting thin plates. *Appl. Phys. Lett.* **94**, 242501 (2009). doi:10.1063/1.3154555

18. A. Sanchez, C. Navau, J. Prat-Camps, D.-X. Chen, Antimagnets: Controlling magnetic fields with superconductor–metamaterial hybrids. *New J. Phys.* **13**, 093034 (2011). doi:10.1088/1367-2630/13/9/093034

19. J. J. Rabbers, M. P. Oomen, E. Bassani, G. Ripamonti, G. Giunchi, Magnetic shielding capability of MgB_2 cylinders. *Supercond. Sci. Technol.* **23**, 125003 (2010). doi:10.1088/0953-2048/23/12/125003

20. Y. Xie, K. Tekletsadik, D. Hazelton, V. Selvamanickam, Second generation high-temperature superconducting wires for fault current limiter applications. *IEEE Trans. Appl. Supercond.* **17**, 1981 (2007). doi:10.1109/TASC.2007.898186

21. Materials and methods are available as supporting material on *Science* Online.

22. M. Solovyov, F. Gömöry, Study of YBCO tape non-uniformity based on the AC loss and the magnetic field distribution in current transport. *IEEE Trans. Appl. Supercond.* **21**, 3277 (2011). doi:10.1109/TASC.2010.2086998

23. J. Vrba, S. E. Robinson, Signal processing in magnetoencephalography. *Methods* **25**, 249 (2001). doi:10.1006/meth.2001.1238 Medline

24. H. Chen, C. T. Chan, P. Sheng, Transformation optics and metamaterials. *Nat. Mater.* **9**, 387 (2010). doi:10.1038/nmat2743 Medline

25. V. M. Shalaev, Transforming light. *Science* **322**, 384 (2008). doi:10.1126/science.1166079 Medline

26. U. Leonhardt, To invisibility and beyond. *Nature* **471**, 292 (2011). doi:10.1038/471292a Medline

27. C. P. Bean, Magnetization of hard superconductors. *Phys. Rev. Lett.* **8**, 250 (1962). doi:10.1103/PhysRevLett.8.250

28. F. Gömöry, M. Vojenciak, E. Pardo, J. Souc, Magnetic flux penetration and AC loss in a composite superconducting wire with ferromagnetic parts. *Supercond. Sci Technol.* **22**, 034017 (2009). doi:10.1088/0953-2048/22/3/034017

29. F. Gömöry, M. Vojenciak, E. Pardo, M. Solovyov, J. Souc, AC losses in coated conductors. *Supercond. Sci Technol.* **23**, 034012 (2010). doi:10.1088/0953-2048/23/3/034012

30. J. D. Jackson, *Classical Electrodynamics* (Wiley, New York, ed. 3, 1999).

31. G. W. Milton, *The Theory of Composites* (Cambridge Univ. Press, Cambridge, ed. 1, 2002).

32. Z. Hashin, The elastic moduli of heterogeneous materials. *J. Appl. Mech.* **29**, 143 (1962). doi:10.1115/1.3636446

33. M. Kerker, Invisible bodies. *J. Opt. Soc. Am.* **65**, 376 (1975).